A study on coordination between a line of sight and motion of body during hitting a ball with a racket

Toshikazu Yagi*, Satoru Kizawa, and Ayuko Saito

Department of Mechanical Science and Engineering, School of Advanced Engineering, Kogakuin University, Tokyo, Japan
E-mail: your_s518066@ns.kogakuin.jp

Abstract
investigate the coordination between a line of sight and motion of body during hitting a ball with a racket. As a result The result was different with or without instructions.

Integrating the information on visual, vestibular sense, and proprioception, and perceiving them are important to control human motion. Vision is the sense which perceives the external environment. Vestibular is the sense which perceives the inclination of the body. Proprioception is the sense of self-movement and body position. A person integrates those senses to sustain a standing position. Vision is different from other senses because it is a sense which obtains information about the external environment away from the body. When humans move their bodies in daily life or exercise, recognizing the positional relationship between space and destination using vision is needed. Analyzing coordination between the visual and body-sense systems contributes to improve the efficiency of sports practice and instruction. We focused on the movement of the line of sight during hitting a ball with a racket. A gaze measurement system and an optical motion capture were used in the experiment. A gaze measurement system converted the center position of the pupil to two-dimensional coordinates. An optical motion capture was used to measure the upper limb joint angles. The coordination between the line of sight and upper limbs of a person hitting a ball is examined by applying singular value decomposition [1][2]. Furthermore, we verify the result for the condition in which the thrower throws a ball after stating the direction in which the ball will be passed. We also verify the result for the condition in which the thrower throws the ball without stating the intended direction. This allows us to verify the difference in visual-motor coordination of a player depending on the presence or absence of advance notice of the direction in which he or she needs to move.

The line-of-sight positions were acquired using a gaze measurement system. The upper limb joint angles were measured using an optical 3D motion capture system. The positions of reflective markers for the motion capture system were determined by reference to the Helen Hayes marker set. The definitions of upper limb joint angles are shown in Table 1. The definitions of shoulder joint angles and elbow joint angles are shown in Figs. 1 and 2 respectively. The player’s line-of-sight positions were obtained as pixel coordinates on the visual field plane (X-Z plane) shown in Fig. 3. The horizontal X-axis ranged from -319 pixels to 319 pixels. The vertical Z-axis ranged from -239 pixels to 239 pixels. healthy adult (height 1.63m, weight 53.0 kg) participated in the experiment. After receiving an explanation of the purpose and requirements of the study, the participant gave his written informed consent to participate. Study approval was obtained from the Research Ethics Board, National Institute of Technology, Kogakuin University (Approval number 2020-B-1).

The reference coordinate system in the laboratory and the standing positions of a thrower and a player are shown in Fig. 4. They stood 2.7 m apart on the Y-axis of the reference coordinate system. The thrower was instructed to throw the ball 5 seconds after the thrower’s signal. The direction to throw the ball was

Fig.1 Definitions of upper limb joint angles.

Angles	Associated movement	Angles	Associated movement
Left shoulder angle (LSX)	Flexion	Right shoulder angle (RSX)	Flexion
Left shoulder angle (LSY)	Abduction	Right shoulder angle (RSY)	Abduction
Left shoulder angle (LSZ)	Internal rotation	Right shoulder angle (RSZ)	Internal rotation
Left elbow angle (LE)	Flexion	Right elbow angle (RE)	Flexion

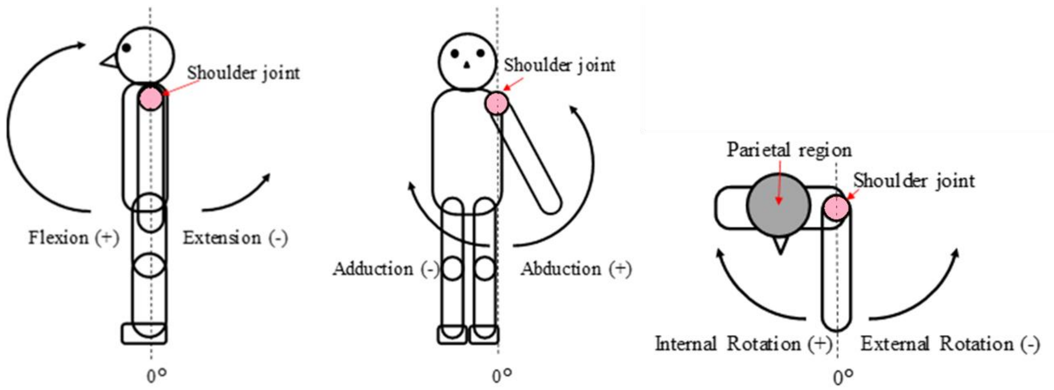

(a) Flection-Extension *(b)Abduction-Adduction* *(c)Internal Rotation-External Rotation*

Fig. 1 Definitions of shoulder joint angles.

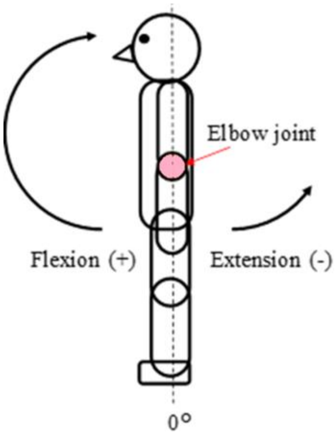

Fig. 2 Definitions of elbow joint angles.

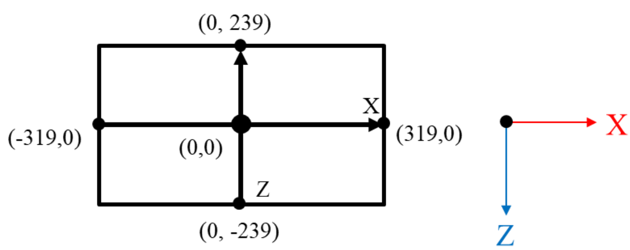

Fig. 3 Definition of pixel coordinate system.

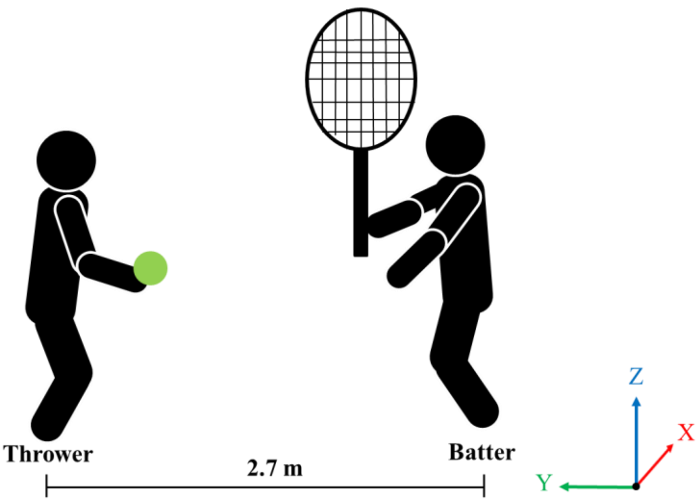

Fig. 4 Definition of the reference coordinate system and standing positions.

to either the right or left side of the batter. The thrower held the ball in his right hand, and threw the ball using an underhand toss in all trials. The experiment aimed to confirm visual-motor coordination from the common features of the results of repeated similar movements by the player. Thus, we conducted two trials under each condition. The trials, in which the thrower threw the ball after stating the intended direction the ball, were performed twice each on the left and right sides. Then, trials in which the thrower tossed the ball without stating the intended direction were performed twice each on the left and right sides. Because the purpose of this study was to analyze visual-motor coordination of basic motion as a ball is hit, the player was instructed to maintain a standing position and hit the ball without moving his feet to eliminate complicated motions. Sampling frequencies of the gaze measurement system and the optical motion capture system were each 60 Hz.

Upper limb joint angles and pixel coordinates of the line-of-sight positions were converted into dimensionless quantities of -1 to 1 as follows:

$$\theta(t) = \frac{2(\theta_{raw}(t) - \theta_{min})}{\theta_{max} - \theta_{min}} - 1 \qquad (1)$$

where $\theta(t)$ represents the normalized joint angles; $\theta_{raw}(t)$ represents the joint angles obtained from an optical 3D motion capture system; θ_{max}, and θ_{min} respectively represent the maximum, and minimum joint angles for each joint. The normalized coordinates of line of sight were calculated in the same way. The observation matrix consists of dimensionless quantities of upper limb joint angles and pixel coordinates of the line-of-sight positions. The observation matrix $R(\theta, G, t)$ is composed as follows:

$$R(\theta, G, t) = \begin{pmatrix} \theta_{LSX}(t_1) & \theta_{LSY}(t_1) & \theta_{LSZ}(t_1) & \theta_{LE}(t_1) & \theta_{RSX}(t_1) & \theta_{RSY}(t_1) & \theta_{RSZ}(t_1) & \theta_{RE}(t_1) & G_x(t_1) & G_z(t_1) \\ \vdots & \vdots & \vdots & \vdots & \vdots & \vdots & \vdots & \vdots & \vdots & \vdots \\ \theta_{LSX}(t_m) & \theta_{LSY}(t_m) & \theta_{LSZ}(t_m) & \theta_{LE}(t_m) & \theta_{RSX}(t_m) & \theta_{RSY}(t_m) & \theta_{RSZ}(t_m) & \theta_{RE}(t_m) & G_x(t_m) & G_z(t_m) \end{pmatrix} \qquad (2)$$

where $\theta_{LSX}(t)$, $\theta_{LSY}(t)$, $\theta_{LSZ}(t)$, $\theta_{RSX}(t)$, $\theta_{RSY}(t)$, and $\theta_{RSZ}(t)$ respectively represent the angles of flexion, abduction, and internal rotation in the left and right shoulders; $\theta_{LE}(t)$ and $\theta_{RE}(t)$ respectively represent the angles of flexion in the left and right elbows; $Gx(t)$ and $Gz(t)$ respectively represent the pixel coordinates of the line-of-sight positions for the x and z axes in consideration of the flexion, extension, internal rotation, and external rotation of the subject's head; and m represents the number of time-series data points.

The observation matrix [Eq. (2)] is decomposed into the basis vectors as

$$R(\theta, G, t) = \sum_{j=1}^{n} \lambda_j V_j(t) Z_j^T(\theta, G)$$
$$(j = 1, \ldots, n, \quad n = 10) \qquad (3)$$

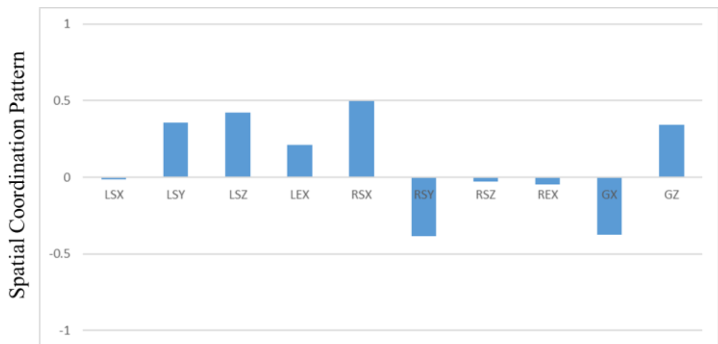

(a) The first mode.

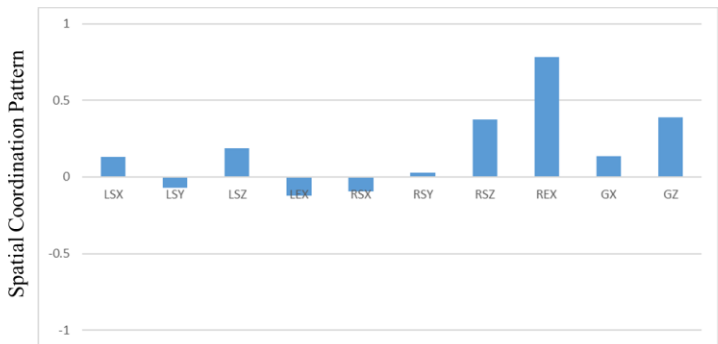

(b) The second mode.

Fig. 5 Spatial coordination pattern of the lines of sight and upper limb joint angles when the thrower threw the ball after stating the throwing direction.

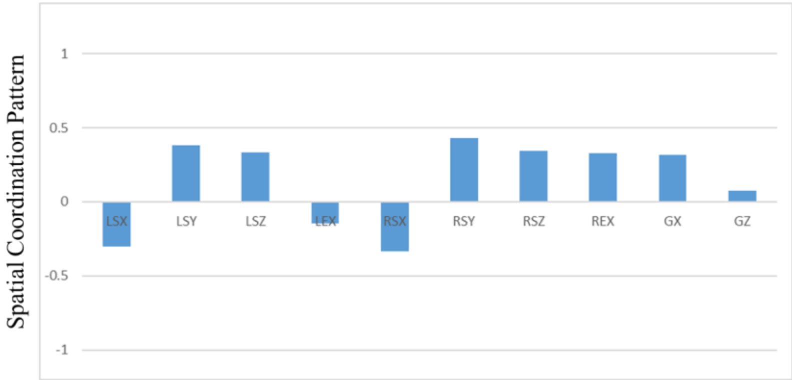

(a) The first mode.

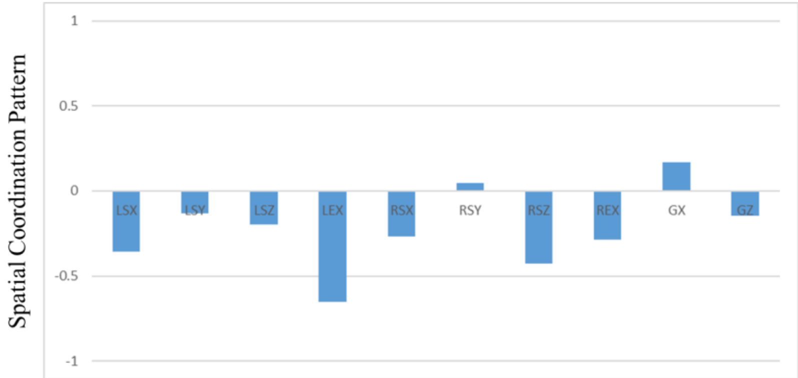

(b) The second mode.

Fig. 6 Spatial coordination pattern of the lines of sight and upper limb joint angles when the thrower threw the ball without stating the throwing direction.

where λ_j is a singular value. The motion modes are defined in descending order of λ_j.

The contribution ratio β_j of the singular value in the *j*-th motion mode is

$$\beta_j = \frac{\lambda_j}{\sum_{j=1}^{n} \lambda_j^{\,2}} \quad (j = 1, \ldots, n,\ \ n = 10) \tag{4}$$

where *j* is the number of columns in the observation matrix.

The contribution ratio of the first mode was calculated to be about 40%, the second mode 20%, and the third and later modes less than 10% in all trials of the subject. Consequently, we concluded that the first mode was the dominant motion mode in each trial. The second mode accounted for about 20% of the motion, including characteristic coordination patterns. Therefore, the results for the first and second modes were examined in detail.

The spatial basis results, which represent the coordination patterns, are shown in Figs. 6 and 7. Figure 6 is the results of the trial in which the thrower tossed the ball to the subject's right side after stating the intended direction. Figure 6 is the result of the trial in which the thrower tossed the ball to the subject's right side without stating the intended direction. In Figs. 6 and 7, panel (a) provides the result for the first mode; panel (b) presents the second mode.

References:

[1] Funato, T., Aoi, S. and Tsuchiya, K., Quantitative evaluation of the intersegmental coordination during human locomotion, Journal of the Robotics Society of Japan, Vol. 28, No. 8 (2010), pp. 996-1003 (in Japanese).

[2] Hayashi, Y., Tsujiuchi, N. and Matsuda, Y., Quantitative evaluation concerning principal gait locomotion pattern of a trans-femoral amputee with a prosthetic limb based on the intersegmental coordination, Transactions of the JSME (in Japanese), Vol. 81, No. 825 (2015a), DOI : 10.1299/transjsme.15-00020.